

Single-Feed Multi-Beam W-Band Reflectarray for Ultra-Capacity Fixed Wireless Access

Daniel R. Prado, Xuekang Liu, Claudio Paoloni, Rosa Letizia and Lei Wang

School of Engineering, Lancaster University, U.K.

Email: {d.rodriguezprado, x.liu72, c.paoloni, r.letizia, lei.wang}@lancaster.ac.uk

Abstract—A quad-beam reflectarray fed by a single feed horn is designed in W-band at 105 GHz. The feed horn is designed with the goal of being manufactured in a single metallic piece by a CNC milling process. The reflectarray is circular with a periodicity of 0.857 mm and comprised of 15 380 rectangular patches in a single layer of metallization. The four beams are realized by means of the superposition principle and positioned in a great circle corresponding to $(\theta, \varphi) = (30^\circ, 0^\circ)$. The reflectarray is simulated in HFSS modelling each element as a copper patch with a gold coating to avoid corrosion. Simulations show that more than 30 dBi of gain per beam and a gain variation of 1.1 dB are achieved in the frequency range 103 GHz–109 GHz, making suitable for future 6G ultra-capacity fixed wireless access enabled by travelling wave tubes.

Index Terms—Reflectarray, multi-beam, W-band, mm-wave antenna, quad-beam, 6G, fixed wireless access

I. INTRODUCTION

The rapid growth in the number of applications and devices connected to wireless networks [1] has caused the saturation of the sub-6 GHz frequency spectrum, leading to the use of millimetre-wave spectrum for 5G and future 6G new radio networks [2]. Furthermore, with the push to ever higher data rates and traffic, the trend is to move towards higher frequencies in unused bands, such as W- and D-bands, in the sub-THz spectrum [3]. In this regard, one of the main issues of transmitting at sub-THz frequency ranges is the available power. Solid state power amplifiers (SSPAs) can provide less than 1 W of maximum output power at those frequencies [4]. For this reason, only with large, very high gain, expensive and difficult to align antennas the free space path loss as well as the atmospheric losses could be compensated, making links viable only for short distances.

As an emerging solution for higher power at sub-THz frequencies, travelling wave tubes (TWTs) offer wideband behaviour while providing output power that is more than one order of magnitude higher than SSPAs at the same frequency [5]–[7]. This would allow for much smaller antennas, including single-fed multi-beam antennas, reducing visual impact, cost and complexity of the front end.

This work focuses on the design of a single-fed multi-beam reflectarray antenna [8] at 105 GHz in the W-band with the aim of using it in future 6G ultra-capacity fixed wireless access networks with transmission power provided by a TWT. A custom-made horn antenna is designed with the goal of being manufactured in a single metallic piece by a CNC machining process. The horn antenna would be

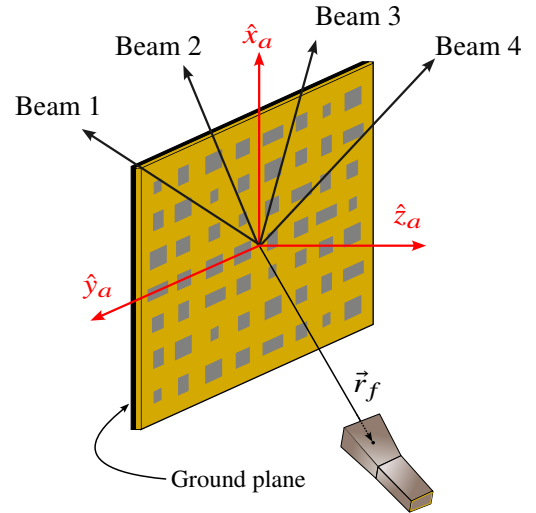


Figure 1. Illustration of a multi-beam planar reflectarray fed by a horn antenna.

connected to a TWT providing the required input power. Then, the reflectarray is designed using in-house software such that it radiates four beams in a great circle. The antenna system (horn and reflectarray) is simulated in Ansys HFSS [9] considering copper patches and a gold coating in the reflectarray elements and ground plane. Simulation results show a minimum gain among all beams of 29.4 dBi and maximum gain variation of 1.8 dBi in the band 102 GHz–109.5 GHz. For the range 103 GHz–109 GHz, the minimum gain is better than 30 dBi with a gain variation of 1.1 dB.

II. ANTENNA DESIGN

A. Definition of the Antenna Geometry

The reflectarray is circular and comprised of 15 380 elements in a regular grid of 140×140 with a periodicity of 0.857 mm, which is 0.3λ at the design frequency, 105 GHz. Thus, the diameter of the reflectarray is 120 mm, or 42λ at the design frequency. A pyramidal horn is used as a feed, whose phase centre is placed at $\vec{r}_f = (-69.1, 0.0, 122.1)$ mm in the reflectarray coordinate system (see Figure 1). The reflectarray is designed to radiate four beams at $(\theta, \varphi) = (31.5^\circ, \pm 19.5^\circ)$ and $(\theta, \varphi) = (39.3^\circ, \pm 45.0^\circ)$. The beams are in a great circle corresponding to $(\theta, \varphi) = (30^\circ, 0^\circ)$.

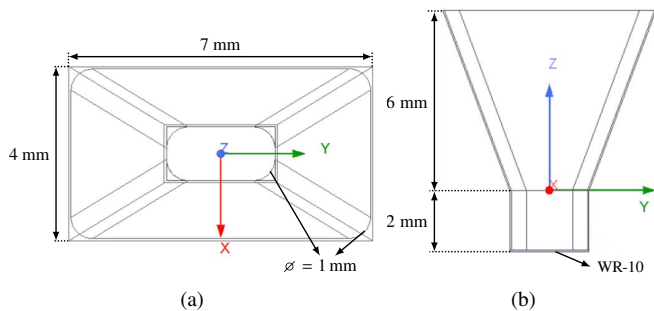


Figure 2. (a) Top and (b) side view of the custom-designed horn antenna for W-band operation. For practical manufacturing purposes, there is a chamfer with a diameter of 1 mm.

B. Feed Horn Design

The feed antenna is a custom-made pyramidal horn, specifically optimized for CNC machining to produce the entire antenna as a single unit. During the design process, the dimensions and structure were carefully adjusted to accommodate the manufacturing technique. For example, to ensure the antenna could be machined as a single piece, the overall length was limited to less than 10 mm. Additionally, the inner edges of the antenna were chamfered. As shown in Figure 2, the top and side views of the antenna have an aperture size of 7 mm by 4 mm. The chamfered corners have a diameter of 1 mm, while the WR-10 waveguide section is 2 mm long, and the flare section extends 6 mm. The waveguide will be connected to the TWT, which provides the input signal.

Figure 3 shows the simulated radiation patterns of the horn antenna at 105 GHz. The main cuts of the copolar pattern (CO) are shown for the E- and H-planes, while for the crosspolar pattern (XP) they are for $\varphi = \pm 45^\circ$. The gain of the antenna is 15.2 dBi while the cross-polarization is more than 25 dB below the peak gain. The half-power beamwidths in the E- and H-planes are 36.4° and 28.0° , respectively.

C. Reflectarray Design

The chosen unit cell is comprised of a single rectangular patch in one layer of metallization backed by a ground plane, as shown in Figure 4(a). An efficient and flexible in-house method of moments in the spectral domain employing basis functions based on Chebyshev polynomials with edge singularities [10] has been developed to analyse this unit cell. A F4BME300 substrate is employed in the simulations, with parameters $\epsilon_r = 3.0$, $\tan \delta = 0.0025$ and $h = 0.127$ mm. Figure 4(b) shows the phase-shift response of this unit cell for various angles of incidence at 105 GHz and various frequencies for ($\theta = 20^\circ$, $\varphi = 20^\circ$). The unit cell offers a phase-shift range of approximately 295° , as well as a good angular stability. The limitation in the phase-shift range will be taken into account for the layout design.

To achieve the multi-beam capability, phase superposition [11] is applied. First, for each beam l and reflectarray element

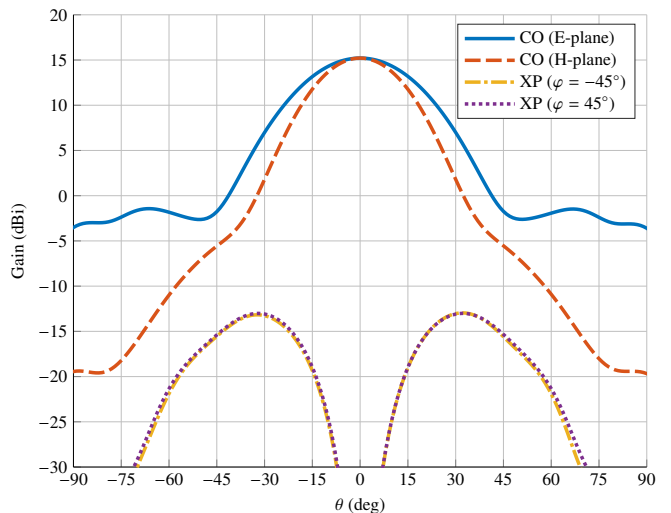


Figure 3. Main cuts of the radiation pattern of the horn antenna at 105 GHz. E- and H-plane correspond to cuts in $\varphi = 0^\circ$ and $\varphi = 90^\circ$, respectively.

i , we find the phase-shift required to point the beam at the far field direction (θ_l, φ_l) with [8]:

$$\angle \rho_{i,l} = \phi_{RA,i,l} - \phi_{inc,i}, \quad (1)$$

where $\phi_{inc,i}$ is the phase of the incident field at the i th reflectarray element, and $\phi_{RA,i,l}$ is the progressive phase distribution that produces a beam pointing at (θ_l, φ_l) :

$$\phi_{RA,i,l} = -k_0 \sin \theta_l \cos \varphi_l x_i - k_0 \sin \theta_l \sin \varphi_l y_i, \quad (2)$$

where k_0 is the free-space wavenumber and (x_i, y_i) are the coordinates of the i th reflectarray element in the reflectarray coordinate system (see Figure 1).

Then, the phase superposition for each reflectarray element is applied with:

$$\tilde{\rho}_i = \sum_{l=1}^L \exp(j \angle \rho_{i,l}), \quad (3)$$

where L is the total number of beams. However, the magnitude of the reflection coefficient $\tilde{\rho}_i$ in (3) is, in general, not one, so it needs renormalization. Thus, the final reflection coefficient will be:

$$\rho_i = \frac{\tilde{\rho}_i}{|\tilde{\rho}_i|}. \quad (4)$$

Figure 5 shows the resulting phase-shift distribution after applying the phase superposition for the desired four beams in a great circle. In addition, a restriction to a range of 295° has been applied to account for the limitation in phase-shift range provided by the unit cell. With this phase-shift distribution, the reflectarray layout is obtained by following the procedure described in [12]. Although the reflectarray has been designed to work in dual-linear polarization, the feed horn will be placed such that the reflectarray will radiate in Y linear polarization according to the diagram presented in Figure 1.

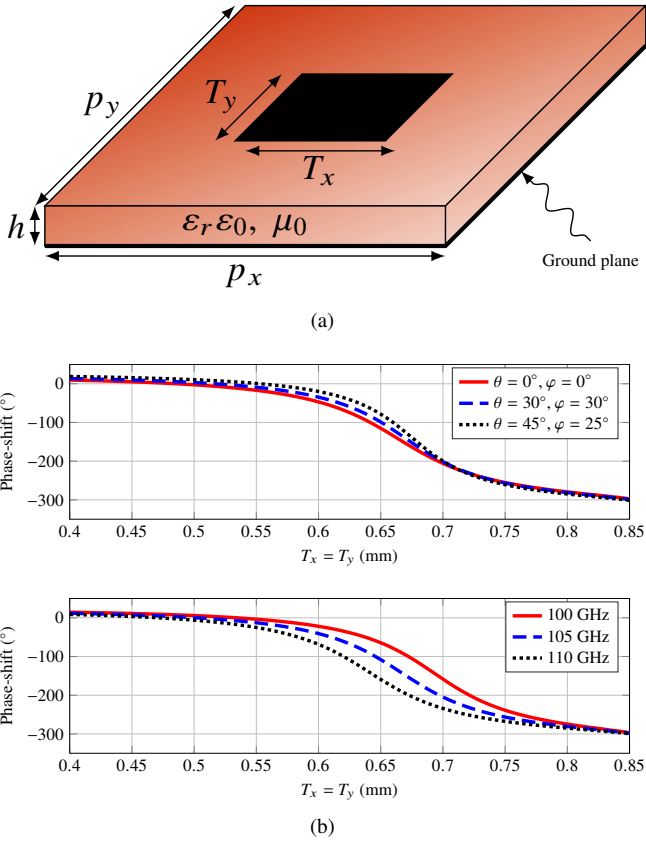


Figure 4. (a) Unit cell consisting of rectangular patch backed by a ground plane. (b) Phase-shift of the unit cell for various angles of incidence at 105 GHz (top) and various frequencies for $(\theta = 20^\circ, \varphi = 20^\circ)$ (bottom).

Figure 6 shows the HFSS setup, where the reflectarray layout can also be seen. The patch sizes vary between 0.427 mm and 0.850 mm. Given that the periodicity of the unit cell is 0.857 mm, the minimum distance between two rectangular patches would be $7 \mu\text{m}$. This distance could be increased by reducing the maximum range in the phase-shift distribution of Figure 5. However, it is still within range for a manufacturing process based on UV photolithography in the university local facilities, which has an accuracy of around $2 \mu\text{m} - 3 \mu\text{m}$.

III. FAR FIELD SIMULATION

A. Simulation Conditions in HFSS

To validate the design procedure of the multi-beam reflectarray, it is simulated in HFSS. To that end, a script to automatically generate an HFSS project file is used, taking around half an hour to generate. In addition, each reflectarray element is composed of two 3D boxes, one below of copper and one on top of gold. The layer of gold is considered to prevent oxidation of the copper from contact with the atmosphere. The ground plane is also comprised of a layer of copper and another of gold. The thickness of each of these layers is $17.399 \mu\text{m}$.

In addition, due to the relative large size of the system horn-reflectarray, it is simulated using hybrid finite-element

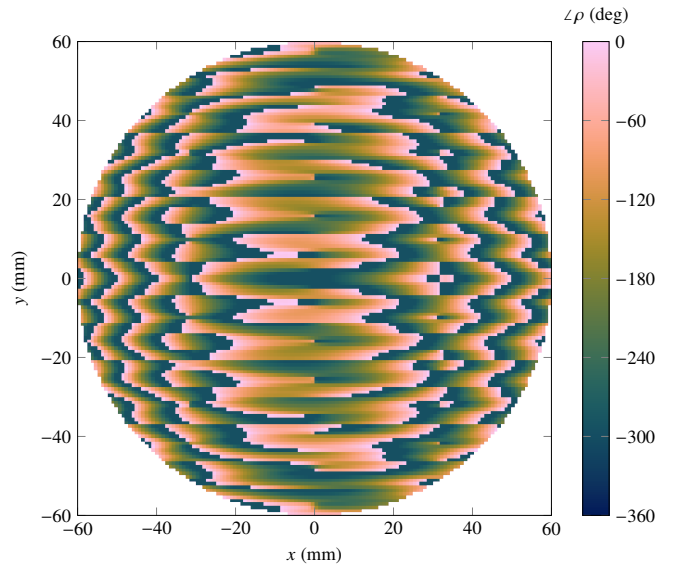


Figure 5. Phase-shift distribution after applying superposition to obtain four beams at 105 GHz in the far field directions $(\theta, \varphi) = (31.5^\circ, \pm 19.5^\circ)$ and $(\theta, \varphi) = (39.3^\circ, \pm 45.0^\circ)$.

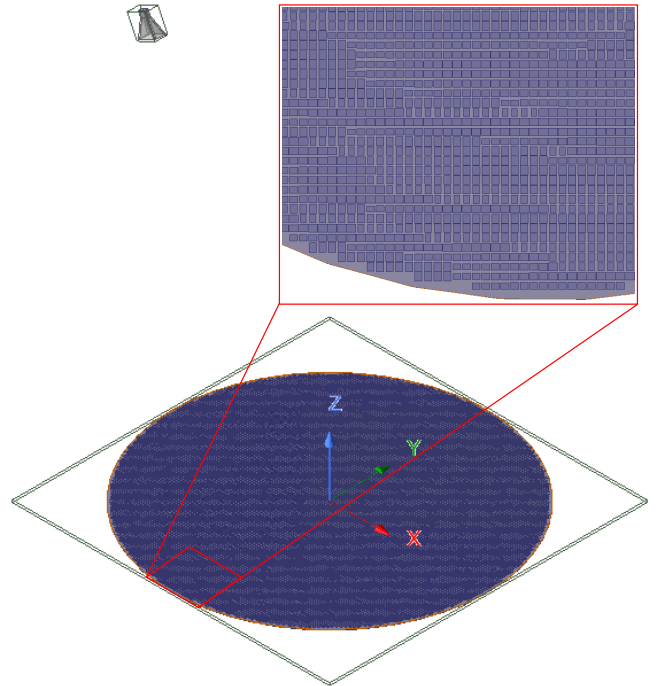


Figure 6. Screenshot of Ansys HFSS showing the feed horn and reflectarray, each surrounded by an air box with hybrid finite-element boundary integral (FE-BI) conditions.

boundary integral (FE-BI) conditions [13], [14]. Figure 6 shows the HFSS setup with FE-BI boxes. The simulation was carried out in a workstation with an Intel Xeon w7-2495X CPU with 512 GB of memory and an NVIDIA RTX A6000 graphics card. It took around 36 h to complete five passes with second order basis functions and with a discrete frequency

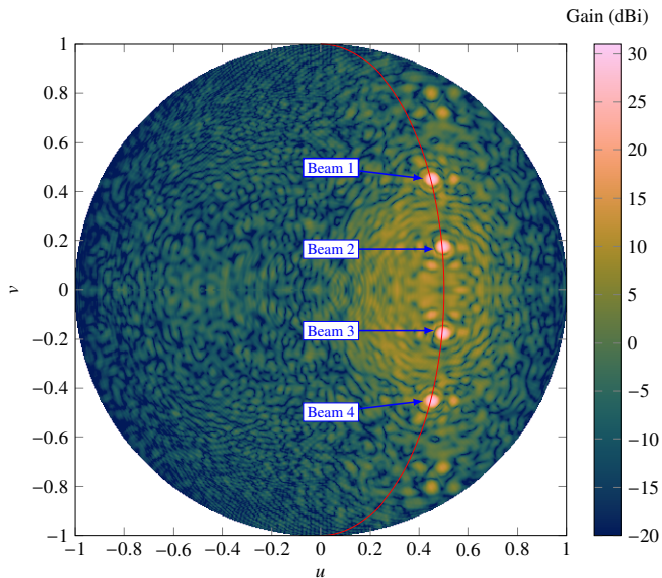


Figure 7. HFSS simulation of the far field copolar component for Y linear polarization at 105 GHz showing the four beams radiated by the reflectarray. The four beams are aligned in the great circle (red solid line) that passes through $(u, v) = (0.5, 0)$, corresponding to $(\theta, \varphi) = (30^\circ, 0^\circ)$.

sweep at nine frequencies in the range 102 GHz–109.5 GHz. In addition to convergence conditions on the S_{11} parameter of the input port in the horn antenna, an extra convergence condition was imposed in the far field gain in the direction of one of the main beams. This is necessary to prevent HFSS from reaching a premature convergence status due to the S_{11} parameter converging much faster than the far field pattern of the whole antenna system. The difference in gain between the last two passes was 0.13 dB.

B. Far Field

Figure 7 shows the 3D copolar pattern for Y linear polarization at 105 GHz simulated with HFSS. The UV grid is defined as $u = \sin\theta \cos\varphi$ and $v = \sin\theta \sin\varphi$, where (θ, φ) are the usual spherical coordinates for the far field. The four beams radiated by the reflectarray lie in the great circle (red solid line) corresponding to $(u, v) = (\sin 30^\circ, 0) = (0.5, 0)$. The gain of the four beams is larger than 30.5 dBi. This can be better appreciated in Figure 8, where the main cuts for different φ planes are shown. Due to the symmetry in the direction of each beam (see Figure 7), beams 1 and 4 are superimposed, as well as beams 2 and 3 in Figure 8. Since the simulation was carried out with assigned materials (copper and gold) for both the horn and reflectarray, the gain already includes metallic as well as dielectric losses.

Finally, Figure 9 shows the gain for each beam in the frequency range of interest in the W-band. All beams have a gain of more than 30 dBi in the range 103 GHz–109 GHz. At 109.5 GHz, beams 1 and 4, which are the beams with the largest θ angle, slightly drop below 30 dBi, while the gain of beam 1 drops below 29.5 dBi at the lowest frequency, 102 GHz. The maximum gain is 31.2 dBi achieved by beam 2

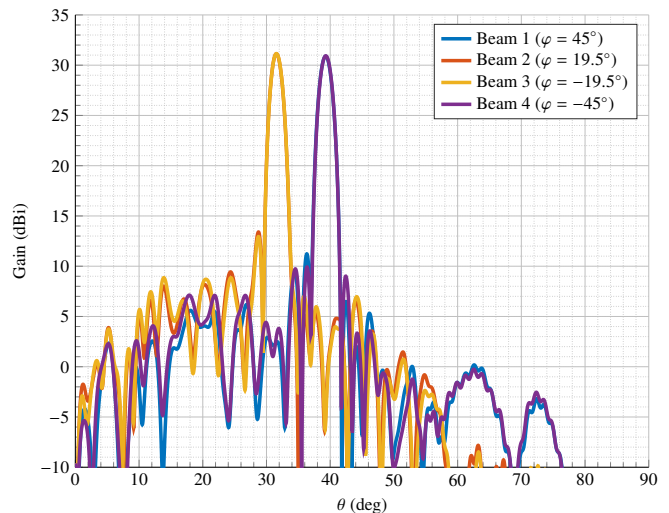


Figure 8. Main cuts of the four beams in θ for different φ planes at 105 GHz. Due to the symmetry in the position of the beams, beams 1 and 4 are superimposed to each other, as well as beams 2 and 3.

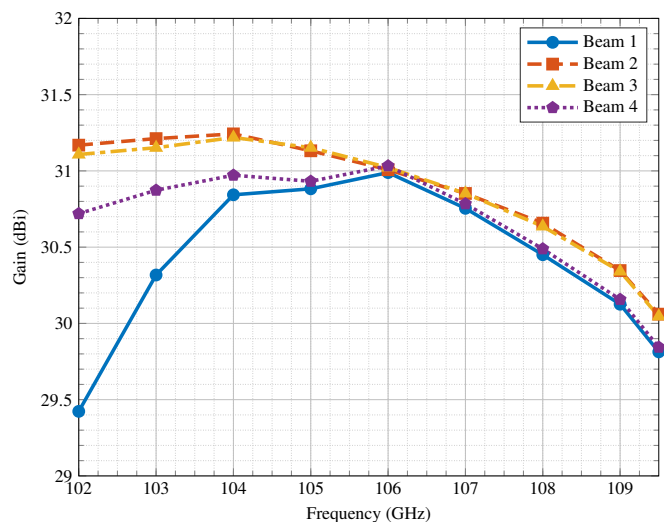


Figure 9. Gain in dBi of the four beams in the frequency range of interest in the W-band.

at 104 GHz, while the minimum gain is 29.4 dBi achieved by beam 1 at 102 GHz. Thus, the total gain variation among all four beams is 1.8 dB in the 102 GHz–109.5 GHz band. In the frequency range 103 GHz–109 GHz the total gain variation is 1.1 dB.

IV. CONCLUSION

A single-fed reflectarray that radiates four beams along a great circle at 105 GHz has been designed and simulated in HFSS. A custom-made horn antenna has been designed with the goal of manufacturing it in a single metallic piece by CNC machining and used as feed for the reflectarray. In order to achieve four simultaneous beams, the phase superposition principle is employed. Then, an in-house method of moments in the spectral domain was employed to obtain the reflectarray

layout. The reflectarray was simulated in HFSS accounting for copper metallizations and a coating of gold to avoid corrosion due to contact with the atmosphere. Simulation results show that each beam provides more than 30 dBi of gain in the frequency range 103 GHz–109 GHz, with a gain variation in that band of just 1.1 dB. In the full band (102 GHz–109.5 GHz), the minimum gain is 29.4 dBi, with a gain variation of 1.8 dB. These results show that reflectarrays are a suitable solution for future 6G ultra-capacity fixed wireless access enabled by travelling wave tubes.

ACKNOWLEDGMENT

This work has been supported by the Innovate UK SBRI: Future Telecommunications Challenge No. 10102343, and by the EPSRC grant EP/Y003144/2.

REFERENCES

- [1] S. Islam, Z. A. Atallah, A. K. Budati, M. K. Hasan, R. Kolandaisamy, and S. Nurhizam, "Mobile networks toward 5G/6G: Network architecture, opportunities and challenges in smart city," *IEEE Open J. Commun. Soc.*, 2024, early access.
- [2] W. Hong *et al.*, "The role of millimeter-wave technologies in 5G/6G wireless communications," *IEEE J. Microw.*, vol. 1, no. 1, pp. 101–122, 2021.
- [3] O. Tervo, I. Nousiainen, I. P. Nasarre, E. Tiirola, and J. Hultkonen, "On the potential of using sub-THz frequencies for beyond 5G," in *Joint European Conference on Networks and Communications & 6G Summit (EuCNC/6G Summit)*, Grenoble, France, Jun. 7–10, 2022, pp. 37–42.
- [4] H. Wang *et al.*, "Power amplifiers performance survey 2000-present," ETH Zürich. [Online]. Available: <https://ideas.ethz.ch/Surveys/pa-survey.html> [Accessed: 16 October 2024]
- [5] C. Paoloni, "Sub-THz wireless transport layer for ubiquitous high data rate," *IEEE Commun. Mag.*, vol. 59, no. 5, pp. 102–107, 2021.
- [6] F. André *et al.*, "Technology, assembly, and test of a W-band traveling wave tube for new 5G high-capacity networks," *IEEE Trans. Electron Devices*, vol. 67, no. 7, pp. 2919–2924, 2020.
- [7] C. Paoloni, R. Basu, P. Narasimhan, J. Gates, and R. Letizia, "Design and fabrication of E-band traveling wave tube for high data rate wireless links," *IEEE Trans. Electron Devices*, vol. 70, no. 6, pp. 2773–2779, 2023.
- [8] J. Huang and J. A. Encinar, *Reflectarray Antennas*. Hoboken, NJ, USA: John Wiley & Sons, 2008.
- [9] "HFSS," Ansys Inc., Pittsburgh, Pennsylvania, USA.
- [10] R. Florencio, R. R. Boix, and J. A. Encinar, "Efficient analysis of multi-resonant periodic structures for the improved analysis and design of reflectarray antennas," in *6th European Conference on Antennas and Propagation (EUCAP)*, Prague, Czech Republic, Mar. 26–30, 2012, pp. 2654–2667.
- [11] J. A. Encinar and J. A. Zornoza, "Three-layer printed reflectarrays for contoured beam space applications," *IEEE Trans. Antennas Propag.*, vol. 52, no. 5, pp. 1138–1148, May 2004.
- [12] D. R. Prado, J. A. López-Fernández, M. Arrebola, M. R. Pino, and G. Goussetis, "General framework for the efficient optimization of reflectarray antennas for contoured beam space applications," *IEEE Access*, vol. 6, pp. 72 295–72 310, 2018.
- [13] P. Naseri, M. Riel, Y. Demers, and S. V. Hum, "A dual-band dual-circularly polarized reflectarray for K/Ka-band space applications," *IEEE Trans. Antennas Propag.*, vol. 68, no. 6, pp. 4627–4637, Jun. 2020.
- [14] J. Silvestro, "Hybrid finite element boundary integral method," Ansys, Canonsburg, Pennsylvania, USA, Tech. Rep., 2010, <https://support.ansys.com> [Accessed: 27 September 2024].